We are IntechOpen,
the world's leading publisher of
Open Access books
Built by scientists, for scientists

6,500
Open access books available

176,000
International authors and editors

190M
Downloads

154
Countries delivered to

Our authors are among the

TOP 1%
most cited scientists

12.2%
Contributors from top 500 universities

CLARIVATE ANALYTICS
BOOK
CITATION
INDEX
INDEXED

WEB OF SCIENCE™

Selection of our books indexed in the Book Citation Index
in Web of Science™ Core Collection (BKCI)

Interested in publishing with us?
Contact book.department@intechopen.com

Chapter

Excited States of Six Anthocyanidin Variants with Different Solvents as Dye Sensitizers for Photocatalysis

Diana Barraza-Jiménez, Hugo Iván Flores-Hidalgo,
Sandra Iliana Torres-Herrera, Raúl Armando Olvera-Corral
and Manuel Alberto Flores-Hidalgo

Abstract

Anthocyanidins in the gas phase and under the effects of solvents such as water, ethanol, n-hexane, and methanol have been studied using DFT and TDDFT electronic structure calculations for applications as natural dyes in photocatalysis. The results include HOMO and LUMO orbitals, HOMO-LUMO gap, chemical properties, reorganization energies, and excited states. Malvidin presented the lower HOMO-LUMO gap energy. After the inclusion of solvents, HOMO-LUMO gap energy increased in all cases, presenting malvidin with n-hexane as the narrower gap energy. Conceptual DFT results showed that cyanidin, malvidin, and pelargonidin present good charge transfer properties. Cyanidin presented a lower electron reorganization energy (λ_e) when water is used as the solvent. TDDFT has been used for excited states calculation and absorption data show the main peaks in a wavelength between 479.1 and 536.4 nm. The UV–Vis absorption spectra were generated and the solvent effects in each case are discussed. In consequence, pigments selected in this attempt are suitable to work in the visible part of the electromagnetic spectrum and display the main peak in the green region. These pigments are found as good options for photocatalysis applications, and the best choices for dye sensitization are cyanidin, malvidin, and petunidin after including the more common anthocyanidins in the analysis.

Keywords: anthocyanidins, Dyes, DSSC, TDDFT, conceptual DFT

1. Introduction

Dye-sensitized solar cell (DSSC) is a promising photovoltaic technology and part of several green technologies used for environmental remediation based on taking advantage of sunlight as the energy source. The number of researchers dedicated to working on the development of this technology has increased exponentially in late years [1]. An important part of this technology relates to dyes which are used to sensitize the semiconductor in DSSCs. The development of new more efficient dyes is

part of the research trends to improve this technology [1–3]. Natural pigments represent one of the more important choices to have improved dyes in DSSCs.

DSSCs discovery by Michael Grätzel and Brian O'Regan is dated in 1991 [4]. This device is a photoelectrochemical cell that imitates the photosynthesis process in plants. The cell consists of a semiconductor-based photoanode covered with a dye layer, a summarized functioning of the device is described as follows to understand the dye's role and importance in a DSSC [5, 6]. Dye photoexcitation provides an electron injection into the semiconductor conduction band from the dye LUMO which is caused by energy bands overlap. Next, the oxidized dye is regenerated when an electron is given up from the redox electrolyte. Electrolyte species reduction is completed with the addition of an electron at the platinum-coated transparent conducting oxide (TCO). The remainder of the semiconductor Fermi level and the electrolyte redox potential is equivalent to the open-circuit voltage [7, 8].

The idea of using the reactions of photosynthesis to convert sunlight into electrical power was published in 1974 by Melvin Calvin and became a common technique in solar technology [9–11]. Solar cells started with silicon devices, but technology has advanced, and new materials and devices were created, this progress includes DSSCs as part of an emerging third-generation photovoltaic concept in which stands out the use of synthetic or natural dyes as light-harvesting pigments [5, 6]. DSSCs components require more research and development to reach higher efficiencies [12–14]. Photosensitizers based on natural pigments are more desirable in DSSCs than dyes from metal complexes and may reach similar performances and stability [9]. Our interest within this work relates to natural pigments' electronic structure and will be focused on anthocyanidins.

Selected pigments are among the more commonly found anthocyanidins in nature, six different aglycones or anthocyanidins are included within this work and its common name with its distribution in fruits and vegetables is as follows: cyanidin 50%, pelargonidin 12%, delphinidin 12%, peonidin 12%, petunidin 7%, and malvidin 7% [15–18]. Hydroxyl and methoxy groups differentiate these molecules by the number and position of their B-ring [19–21]. Prior work related to anthocyanidins by our research group has been published elsewhere and includes cyanidin, malvidin, and peonidin [22]. The methodology from such work was reproduced with an upgraded version of the Gaussian program as part of the continuity work by our research group and we developed further work with additional pigments and calculations which were included in the present work. This work is considered a deeper study because all calculations were re-done using Gaussian 16 [23] (prior work was developed with G09), in addition, this work includes three additional pigments which enrich twice the options to make the best choice among the more used anthocyanidins for photocatalysis applications. The new calculations not included in the prior work were developed using Cis-TDDFT which enabled an analysis/discussion of emission data and the respective spectra. After increasing to six anthocyanidins in the study, the lower value for gap energy is malvidin in its gas phase and remains as a general behavior that with the addition of solvents gap energy increases in all cases except for malvidin with n-hexane because it had the narrower gap followed by petunidin also with n-hexane. For charge transfer, based on conceptual DFT results, cyanidin, malvidin, and pelargonidin present the best results. Water as solvent followed by ethanol and methanol applied in cyanidin displayed the lower values for electron reorganization energy (λ_e). Also, TDDFT calculations were carried out to calculate absorption properties for each pigment. After increasing the sample from three

molecules up to six, it was again cyanidin, malvidin, and petunidin the pigments with the best performance indices for dye sensitization.

2. Theory and computational details

Theoretical calculations were performed in Gaussian16 (G16) programs suite [23]. Calculations include four solvents (water, ethanol, n-hexane, and methanol) in addition to the gas phase. Selection criteria are mainly based on how often the solvent is used in the laboratory to obtain pigments. The solvation model was PCM (polarizable continuum solvation model) as implemented in G16 program suite. B3LYP/6–311 + g (d,p) is the theoretical method used during geometry relaxation. Open-source databases were used to obtain the first geometry version and then our theoretical methodology was applied to optimize geometric parameters. Functional B3LYP is a widely accepted approach for this kind of molecule, and it was selected for this study mainly for that reason [24]. Basis set 6–311 + g(d,p) as implemented in the Gaussian16 program package [23] complements B3LYP very well according to preliminary calculations. 6–311 + g(d,p) was tested by running a set of calculations with different organic molecules with more than acceptable results. The literature considers B3LYP/ 6–311 + g(d,p) a theoretical method that provides a good level of accuracy for similar molecules [25–29]. A local minimum needs to be reached at the geometric optimization and it was confirmed with the calculation of harmonic vibrational frequencies. The zero-point vibrational energy (ZPVE) scaling was performed as a thermal correction (TC) at 298.15 K. Complementing geometry and frequency calculations, neutral energy, and adiabatic energies were obtained. Thereupon, chemical properties (HOMO, LUMO, gap, ionization potential (IP), electronic affinity (EA), electrophilicity (ω), electronegativity (χ), and hardness (η)) were computed based on the chemical reactivity indexes obtained in energy calculations. The sequence followed during the calculations was: first gas phase and then different solvents, one by one were included such as water, ethanol, n-hexane, and methanol.

Data reported by other research teams were included to compare with our results. So, a good idea is provided on performance against other theoretical methodologies or results obtained experimentally. Discussion is made on whether these molecules may be good dye sensitizers with TiO_2 [25–29] for future work. Excited states were calculated (over 10 states) but only the first excited states will be discussed in this document. TDDFT calculations were carried on with B3LYP/6-311 g + (d,p) for consistency with energy calculations. Useful energy graphs and excited states spectra diagrams considering the six more common anthocyanidin variants in the same figure are included in this work for comparison of results under similar theoretical methods. Chemissian code [30] was used to develop most energy graphs included in the results section.

3. Results and discussion

3.1 Molecular structure

Anthocyanidins are based on the flavylium ion or 2-phenylchromenylium (chromenylium may be referred to as benzopyrylium). These natural pigments are derivatives of 2-phenylchromenylium cation or flavylium cation. A relevant feature

for this structure is the capability to carry different substituents in the phenyl group at 2-position. Another particularity to note is anthocyanidins differ from other flavonoids because of a positive charge. Molecule substituents and main features are displayed in **Table 1** which includes a molecular scheme in **Figure 1** shown next to the table so the reader may have a good view for a general interpretation of structural differences between anthocyanidin variants. Anthocyanidins have a 15-carbon atoms main structure arranged in two aromatic rings (A and B) as shown in **Figure 1**. A third ring (C) provides the positive charge from an oxygen atom contained in this ring. Two C=C bonds in the C ring differentiate anthocyanidins among the flavonoid family and it is responsible for a positive charge in this molecule, therefore, it is a cation (flavylium) when it is at the stable form at low pH [31].

The phenylbenzopyrylium core of anthocyanins may be modified by the addition of a wide range of chemical groups using hydroxylation, acylation, and methylation.

Geometric parameters are summarized in **Table 2**. The phenylbenzopyrylium is normally combined with a wide range of chemical groups using hydroxylation, acylation, and methylation.

The C—C bond length found within this work has a similar length or nearly enough to 140 pm (C—C bond length average size) which is the typical bond length
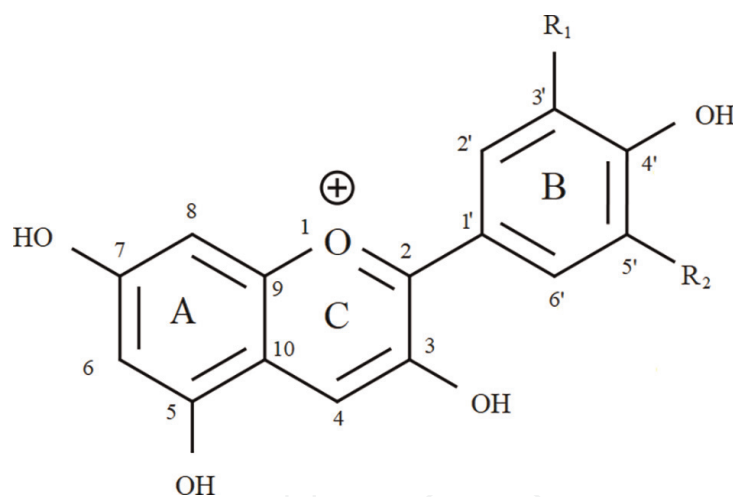

Figure 1.
*General chemical structure of anthocyanidins according to **Table 1**.*

		Substitution pattern		
Name	**Chemical formula**	**R1**	**R2**	**Color**
Cyanidin	$(C_{15}H_{11}O_6)^+$	OH	OH	Orange-red
Delphinidin	$(C_{16}H_{11}O_7)^+$	OH	OH	Blue-red
Malvidin	$(C_{15}H_{13}O_5)^+$	OCH_3	OCH_3	Blue-red
Pelargonidin	$(C_{15}H_{11}O_5)^+$	H	H	Orange
Peonidin	$(C_{15}H_{13}O_6)^+$	OCH_3	H	Orange-red
Petunidin	$(C_{15}H_{12}O_6)^+$	OCH_3	OH	Blue-red

Table 1.
More known anthocyanidins structure and substitution patterns.

Parameter	Cyanidin	Delphinidin	Malvidin	Pelargonidin	Peonidin	Petunidin
O(1)-C(2)	1.350	1.344	1.347	1.345	1.345	1.346
O(1)-C(9)	1.358	1.358	1.359	1.359	1.358	1.359
C(2)-C(3)	1.420	1.403	1.407	1.404	1.404	1.406
C(2)-C(1′)	1.436	1.448	1.444	1.445	1.447	1.446
C(3)-C(4)	1.382	1.390	1.388	1.389	1.390	1.390
C(4)-C(10)	1.403	1.397	1.399	1.397	1.397	1.398
C(5)-C(6)	1.376	1.375	1.376	1.375	1.375	1.375
C(5)-C(10)	1.427	1.436	1.435	1.436	1.436	1.436
C(6)-C(7)	1.412	1.409	1.408	1.409	1.409	1.409
C(7)-C(8)	1.395	1.399	1.398	1.399	1.398	1.398
C(8)-C(9)	1.386	1.380	1.382	1.381	1.381	1.382
C(9)-C(10)	1.409	1.423	1.421	1.422	1.423	1.422
C(1′)-C(2′)	1.422	1.406	1.414	1.415	1.409	1.414
C(1′)-C(6′)	1.414	1.416	1.407	1.413	1.411	1.410
C(2′)-C(3′)	1.377	1.389	1.381	1.377	1.387	1.385
C(3′)-C(4′)	1.422	1.404	1.418	1.405	1.420	1.409
C(4′)-C(5′)	1.396	1.403	1.407	1.403	1.399	1.401
C(5′)-C(6′)	1.383	1.386	1.395	1.383	1.384	1.389
O(1)-C(2)-C(1′)-C(6′)	180	150.1	151.4	150.5	150.1	150.6
C(3)-C(2)-C(1′)-C(2′)	180	148.5	149.3	149.8	149.1	148.3
O-C(3′)-C(4′)-C(5′)	180	179.9	179.3	180.0	177.4	179.9
H-C(5′)-C(4′)-C(3′)	180	178.2	175.9	177.9	178.5	178.2
O-C(4′)-C(3′)-C(2′)	180	179.7	177.0	179.9	176.7	179.8
O-C(4′)-C(5′)-C(6′)	180	179.2	178.0	179.3	177.7	179.4
C(8)-C(9)-C(10)-C(4)	180	175.7	176.3	175.6	175.9	176.2
O(1)-C(9)-C(10)-C(5)	180	178.6	178.8	178.6	178.7	178.8
C(8)-C(9)-O(1)-C(2)	180	179.0	179.9	179.1	179.4	179.6
C(5)-C(10)-C(4)-C(3)	180	179.7	179.3	179.7	179.5	179.4
C(9)-O(1)-C(2)-C(1′)	180	179.4	179.1	179.0	179.0	179.3

*Data regenerated by our research group with a similar theoretical method reported elsewhere [22].

Table 2.
Selected anthocyanidins geometric parameters summary including bond length and bond angles in Å and °,
respectively.

for benzene. An average of 154.0 pm and 134 pm were found for single and double C—C bonds length, respectively. C—C bond lengths for benzene are customarily accepted around 139 pm in the literature which is near to our findings. The discrepancy is minor near to 0.1 Å in average for C—C bonds of selected pigments considering an average length between 1.346 and 1.444 Å.

Methodologies such as B3LYP/6-31 g(d), B3LYP/6–31 + g(d,p) have been reported in the literature for similar molecules [32–36] and will be included a few selected data from some of these sources to enrich the discussion in this work. At his point, one can say B3LYP reaches accurate results for these molecules' geometries and may be expected good results for similar organic molecules as well. Thus, results in this work for C—C bond lengths comply with the reported data.

The planarity in a structure is related to dihedral angles. For anthocyanidins within this work, the planarity among the three rings forming these molecules skeleton within each anthocyanidin represents an important feature that differentiates one from another. In the literature, the parameter reported is the torsion angle instead of dihedral angles and this value may be in the same way a factor that characterizes an anthocyanidins and influences its electronic structure behavior [32]. Cyanidin is considered a planar molecule because its dihedrals vary by less than 1° from a perfectly planar structure. Delphinidin and petunidin have similar planarity between them but their torsion angle causes the molecules to have the lower planarity level. Peonidin has more dihedrals different than 180° but only a couple of them differ more than 5°. Then, the analysis indicate there are differences in the dihedrals but only a couple cases deviate significantly from a perfect planarity. However, despite the numeric difference is small, it is such differences in planarity that determine most of the molecule character and its chemical properties. Put it in other words, it may be seen that few dihedrals correspond with a nonplanar structure, in such a way that there is a direct relationship with the relative angle or torsion angle between rings, and it represents the main difference observed in the B ring compared with the rest of the structure. All selected structures fall into the torsion angle and planarity concepts mentioned, with exception of cyanidin which has an almost perfectly planar structure confirmed by its dihedral values.

3.2 Electronic structure

Energy calculations were executed using B3LYP/6311 + g(d,p) method for the gas phase and four solvents (water, ethanol, n-hexane, and methanol). The reader may see HOMO and LUMO molecular orbitals numeric results in **Table 3**. An idea to analyze from these results is how these molecules energy orbitals may overlap with a semiconductor energy orbital for DSSCs and photocatalytic applications.

This procedure consists in reproducing a process where an electron is photo-induced in the molecular system by being transferred from the dye-excited state to the semiconductor. The process takes place at HOMO and LUMO energy orbitals. Therefore, a dye sensitizer should have HOMO and LUMO energy levels that mate with electrolyte redox potential and the semiconductor conduction band [25]. Pigments included in this work well with the electrolyte redox level (−4.85 eV) and the conduction band edge for TiO_2 (−4.00 eV), considering values reported in the literature [25–29].

Calculations include molecular orbitals for all variants in the gas phase and with solvents four different solvents. LUMO results are between −6.856 and − 6.624 eV for the gas phase, which is relevant because LUMO molecular orbital may be beneficial for the application as dye sensitizers. An expected condition is dye molecular orbitals overlapping semiconductor band gap in some way so it can take place an easier charge transfer process.

There is a shift around 3 eV in HOMO and LUMO for gas phase results if compared to results when added solvents like water and ethanol. This shift is evidenced in

Pigment	Solvent	H-L	HOMO	LUMO	λ_e	EEP	λ_h	HEP
$(C_{15}H_{11}O_6)^+$	Gas phase	2.664	−9.288	−6.624	0.318	5.525	0.344	10.361
	Water	2.824	−6.452	−3.628	0.262	4.064	0.284	6.038
	Ethanol	2.816	−6.528	−3.712	0.264	4.102	0.288	6.155
	n-hexane	2.712	−7.916	−5.204	0.295	4.818	0.324	8.284
	Methanol	2.818	−6.501	−3.683	0.263	4.089	0.267	6.115
$(C_{16}H_{11}O_7)^+$	Gas phase	2.667	−9.513	−6.846	0.346	5.753	0.364	10.572
	Water	2.844	−6.577	−3.732	0.292	4.191	0.320	6.136
	Ethanol	2.835	−6.658	−3.823	0.294	4.235	0.321	6.260
	n-hexane	2.726	−8.114	−5.388	0.325	5.013	0.346	8.467
	Methanol	2.838	−6.630	−3.792	0.293	4.220	0.320	6.217
$(C_{15}H_{13}O_5)^+$	Gas phase	2.539	−9.24	−6.701	0.371	5.666	0.452	10.162
	Water	2.823	−6.532	−3.709	0.294	4.172	0.460	5.946
	Ethanol	2.810	−6.610	−3.800	0.295	4.216	0.462	6.066
	n-hexane	2.657	−7.975	−5.318	0.335	4.968	0.479	8.169
	Methanol	2.815	−6.583	−3.768	0.294	4.201	0.461	6.024
$(C_{15}H_{11}O_5)^+$	Gas phase	2.881	−9.737	−6.856	0.333	5.732	0.348	10.820
	Water	2.994	−6.693	−3.699	0.290	4.156	0.321	6.250
	Ethanol	2.989	−6.778	−3.789	0.292	4.200	0.322	6.379
	n-hexane	2.918	−8.290	−5.372	0.319	4.984	0.335	8.658
	Methanol	2.990	−6.748	−3.758	0.291	4.185	0.321	6.334
$(C_{15}H_{13}O_6)^+$	Gas phase	2.691	−9.465	−6.774	0.364	5.703	0.498	10.371
	Water	2.955	−6.668	−3.713	0.293	4.173	0.527	6.019
	Ethanol	2.945	−6.748	−3.803	0.294	4.217	0.527	6.142
	n-hexane	2.815	−8.166	−5.351	0.328	4.980	0.533	8.316
	Methanol	2.948	−6.720	−3.772	0.294	4.202	0.527	6.100
$(C_{15}H_{12}O_6)^+$	Gas phase	2.604	−9.379	−6.775	0.341	5.693	0.366	10.411
	Water	2.796	−6.511	−3.715	0.289	4.173	0.318	6.066
	Ethanol	2.785	−6.590	−3.805	0.291	4.216	0.320	6.188
	n-hexane	2.664	−8.014	−5.35	0.318	4.976	0.348	8.353
	Methanol	2.789	−6.562	−3.773	0.290	4.201	0.319	6.145

*Data regenerated by our research group with a similar theoretical method reported elsewhere [22].

Table 3.
Energy results for selected molecules: H-L is the HOMO-LUMO gap or energy band. All units in eV.

HOMO magnitude by around 3 eV. A shift of less than 1.5 eV in HOMO and LUMO is estimated for n-hexane molecular orbitals calculations. The HOMO and LUMO molecular orbitals are shown in **Figures 2** and **3**.

The difference between HOMO-LUMO is generally accepted as a similar value to the band gap. Results for HOMO-LUMO gap were between 2.539 and 2.881 eV in the

Figure 2.
Molecular orbitals for selected anthocyanidins cyanidin [22], delphinidin, malvidin [22], pelargonidin, peonidin [22], and petunidin corresponding to (a) gas phase, (b) water solvent, (c) ethanol solvent, (d) n-hexane solvent and (c) methanol solvent. H-L gap energy units are in eV.

gas phase with malvidin having the narrower gap and pelargonidin with the wider gap among the six pigments.

Therefore, solvents are responsible for a slight shift of HOMO-LUMO values in all cases. Malvidin in the gas phase has a lower value for the HOMO-LUMO energy. With the addition of solvents, these gaps increase in all cases with n-hexane as the narrower value, followed by petunidin also with n-hexane. Ethanol and methanol solvents have a slighter effect than water. In general, effects in HOMO-LUMO are small, which means there is a similarity in magnitude on the results when used any solvent water, ethanol, n-hexane, or methanol. The HOMO-LUMO gap varies in all cases by less than 10% if compared with the HOMO-LUMO values in the gas phase. The greater shift was 11 and 10% corresponding to malvidin and peonidin, respectively, however, n-hexane effect on malvidin shifted only 5%. Then, when water is used a bigger shift in HOMO-LUMO is observed and, in contrast, n-hexane caused the smaller shift. The energy gap had a small variation with ∼0.3 eV on average considering all variants. Cyanidin and delphinidin have alike energy gap values despite the solvent and despite their differences in geometric parameters and constituents. HOMO-LUMO gap energy seems almost unaffected by planarity and relative angles, which means the effects of the main geometric parameters in gap energy are considered small.

There is an amount of energy needed so a molecule can become ionized, which means if one charge is lost it becomes a cation and if one charge is gained it becomes an anion. Such energy was calculated using intramolecular reorganization energies.
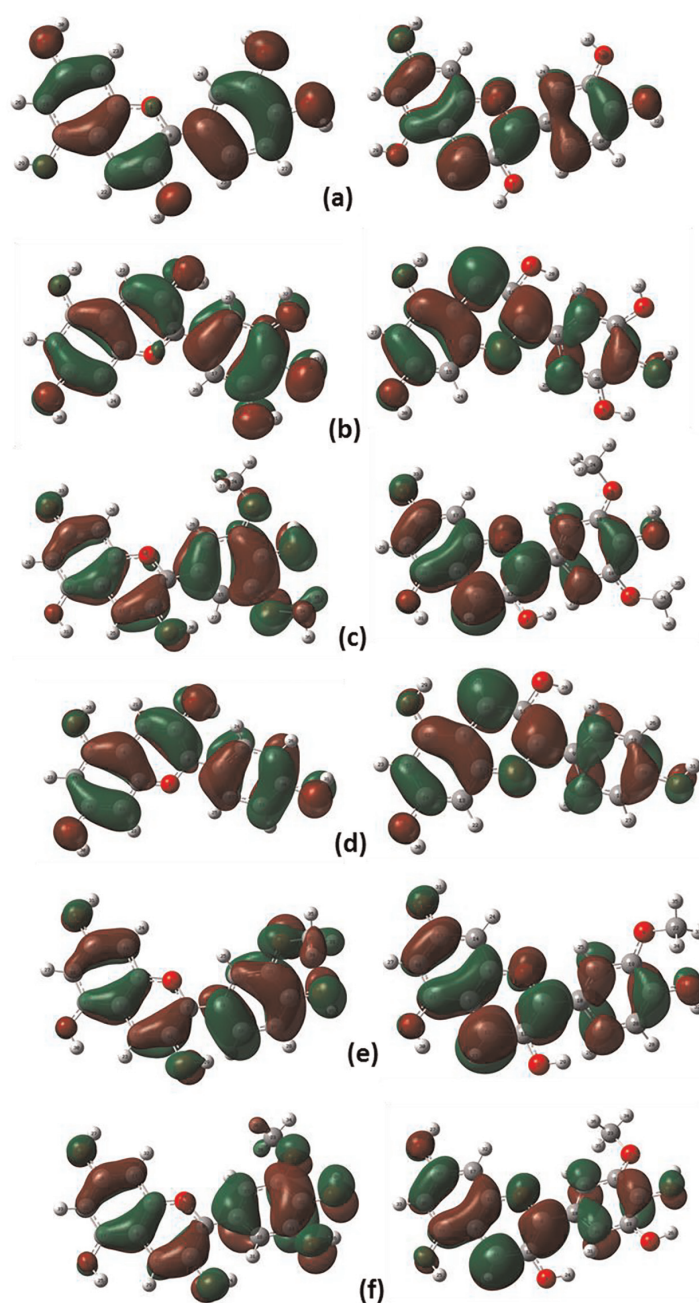
Figure 3.
Molecular orbitals charge distribution using B3LYP/6–311 + g(d,p), corresponding to: (a) cyanidin [22], (b) delphinidin, (c) malvidin [22], (d) pelargonidin, (e) peonidin [22] and (f) petunidin.

When the ionized molecule becomes neutral, then these two processes relate to the charge transfer process. The energy needs to be available for charge transfer for that reason reorganization energy (λ) values are low to prevent wasting energy in reorganization processes. Then, the reason why λ is low is to maximize the use of solar energy instead of using sunlight during the energy transfer process. Water, ethanol, and methanol solvent addition cause a decrease in λ. Solvent n-hexane also decreases λ but slightly. The lower electron reorganization energy (λ_e) was cyanidin with water but with similarities when used ethanol and methanol.

Cyanidin lower hole reorganization energy (λ_h) was obtained when used solvent methanol followed by water with similar values but not as close as in the case of λ_e.

The results for hole extraction potential (HEP) and electron extraction potential (EEP) present higher values for the gas phase, and a decrease is observed when any of the solvents is used.

Water, ethanol, and methanol have a similar effect in HEP and EEP, and it is bigger than n-hexane in all cases. Higher values for HEP were observed in pelargonidin in the gas phase, in general, for gas-phase HEP results are around 10 eV.

With solvent n-hexane, HEP goes around 8 eV and with solvents such as water, ethanol, and methanol its value is nearly 6 eV. EEP values are near 1 eV for solvents water, ethanol, and methanol and go down to 0.5 eV with n-hexane. Higher EEP was observed in delphinidin in the gas phase as expected because of the OH radical present in its molecular structure, but the rest of the selected anthocyanidins had similar values in the gas phase with 0.1 eV variation. Reorganization energies show malvidin is the best choice followed by petunidin.

Cyanidin with methanol produces the best electron reorganization energy λ_e followed by water and ethanol. Cyanidin is more suitable for hole energy λ_h with the same solvents. Petunidin is the next more suitable but with a modest advantage by 0.05 eV over cyanidin. It is possible that λ values performance relates with molecule planarity. The effect of solvents in EEP and HEP is unclear in contrast with λ. Malvidin with water is the best choice from EEP and HEP viewpoint but the variation is minor considering the same solvent is used in other molecules.

3.3 Chemical reactivity properties

Chemical reactivity properties were calculated with conceptual DFT. These properties are shown in **Table 4**.

Ionization potential (IP) is associated with the electronic cloud stiffness. In terms of reactivity, the cloud is wary to become a participant in electron transfer. Therefore, a lower ionization potential is enticing to have a larger molecular potential so electron donation boosts. Malvidin presents the lower IP in its gas phase and decreases further with solvent addition. A similar effect in IP magnitude was caused by water, ethanol, and methanol but the lower IP value was when water is used as a solvent in cyanidin among all variants.

In the gas phase, IP was near 11 eV and when used water, ethanol, and methanol IP decreased to values near 6 eV. IP values also had a reducing trend with solvent n-hexane with results around 8 eV. The lower IP was observed in cyanidin with water and methanol meanwhile for malvidin and petunidin their lower values were observed with these two solvents.

For molecules in its gas phase, EA results were around 5 eV and with solvents water, ethanol, and methanol a reducing trend was observed with results around 3 eV, and n-hexane effect on EA also was a reducing trend to values around 4 eV. Delphinidin in n-hexane has the higher EA but its EA values are only slightly higher than those for pelargonidin, petunidin, peonidin, and malvidin, all with n-hexane.

Attracting electron pairs may be measured with electronegativity (χ). For a better suitability to act as a charge acceptor, a high electronegativity (χ) is desirable. Pelargonidin displayed the highest χ value in the gas phase, in general χ results are near 8 eV and have a decreasing trend with values near 5 eV when solvents such as water, ethanol, and methanol are used. For n-hexane solvent, results are near 6 eV. Pelargonidin with n-hexane presents the higher value but it is slightly over the rest of the molecules using n-hexane as well.

Pigment	Solvent	IP	EA	χ	η	ω	S
$(C_{15}H_{11}O_6)^+$	Gas phase	10.642	5.154	7.898	2.744	11.439	0.364
	Water	6.322	3.802	5.062	1.26	10.165	0.793
	Ethanol	6.443	3.838	5.141	1.302	10.147	0.768
	n-hexane	8.608	4.522	6.565	2.043	10.549	0.490
	Methanol	6.382	3.825	5.104	1.278	10.189	0.782
$(C_{16}H_{11}O_7)^+$	Gas phase	10.876	5.353	8.114	2.761	11.923	0.362
	Water	6.456	3.899	5.177	1.278	10.485	0.782
	Ethanol	6.582	3.941	5.261	1.320	10.484	0.757
	n-hexane	8.813	4.688	6.751	2.062	11.048	0.485
	Methanol	6.537	3.927	5.232	1.305	10.485	0.766
$(C_{15}H_{13}O_5)^+$	Gas phase	10.614	5.296	7.955	2.659	11.899	0.376
	Water	6.406	3.878	5.142	1.264	10.462	0.791
	Ethanol	6.528	3.921	5.224	1.304	10.469	0.767
	n-hexane	8.647	4.633	6.640	2.007	10.983	0.498
	Methanol	6.486	3.906	5.196	1.29	10.466	0.775
$(C_{15}H_{11}O_5)^+$	Gas phase	11.181	5.399	8.29	2.891	11.886	0.346
	Water	6.571	3.866	5.219	1.352	10.07	0.739
	Ethanol	6.701	3.908	5.305	1.396	10.077	0.716
	n-hexane	8.992	4.665	6.829	2.164	10.775	0.462
	Methanol	6.656	3.894	5.275	1.381	10.074	0.724
$(C_{15}H_{13}O_6)^+$	Gas phase	10.869	5.34	8.105	2.765	11.879	0.362
	Water	6.545	3.881	5.213	1.332	10.199	0.751
	Ethanol	6.670	3.922	5.296	1.374	10.209	0.728
	n-hexane	8.850	4.652	6.751	2.099	10.859	0.477
	Methanol	6.627	3.908	5.267	1.359	10.205	0.736
$(C_{15}H_{12}O_6)^+$	Gas phase	10.777	5.352	8.064	2.713	11.987	0.369
	Water	6.384	3.884	5.134	1.25	10.541	0.8
	Ethanol	6.508	3.925	5.217	1.291	10.536	0.774
	n-hexane	8.701	4.658	6.679	2.022	11.034	0.495
	Methanol	6.465	3.911	5.188	1.277	10.537	0.783

[*]*Data regenerated by our research group with similar theoretical method reported elsewhere [22].*

Table 4.
Chemical reactivity of selected anthocyanidins. Properties displayed are ionization potential (IP), electron affinity (EA), electronegativity (χ), chemical hardness (η), electrophilicity index (ω), and chemical softness (S), units are eV.

Therefore, chemical properties show similarity among resulting values which may be induced by the molecular resemblances including the torsion angle, and the small structural differences may be responsible for the main differences as well as their molecule constituents.

3.4 Excited states with TDDFT

TDDFT excited states were computed with B3LYP/6311 + g(d,p) methodology in Gaussian16. The literature supports that B3LYP is a suitable hybrid functional [25–29, 36] for this kind of computations and has been successful in similar molecules.

A good match between the absorption spectrum and the solar irradiation spectrum in DSSCs benefits its performance. An indicator of the light-harvesting effectiveness may be data related to the dye's absorption and such data become relevant for the performance of the DSSCs [37–41] as a whole. Our results are in acceptable accord with experimental values and the differences may be caused by solvent effects and variation added by measuring methodologies [36, 42–44]. For ΔE, a low value is desirable so the first excited state may need as low energy as possible. In the gas phase, malvidin presents the lower value for ΔE and, with solvent addition, the lower value was malvidin with n-hexane closely followed by petunidin with n-hexane. The literature reports two main regions in anthocyanidins UV–Vis spectra. The first one at 260–280 nm and the second one at the visible region between 490 and 550 nm. There is a third peak at 310–360 nm [43], but we will focus on the main peak located in the visible region.

This group of anthocyanidins in the gas phase had absorption wavelengths between 479.1 and 536.4 nm. These molecules work in the visible with both cyanidin and pelargonidin working in the blue region. Pelargonidin and malvidin are the lower and higher values while cyanidin presents a similar value with pelargonidin results which may be related to the fact that both have a small relative angle at the B ring and, they are the simplest molecules regarding their constituents. Addition of solvent shifts absorption spectra by increasing its wavelength by less than 5 nm in the case of water, ethanol, and methanol. When used n-hexane, absorption spectra shift by nearly 10 nm. TDDFT excited states absorption data are shown in **Table 5** and absorption spectra are shown in **Figure 4**. Photon-to-current conversion relies on the visible and near UV regions results and based on these results one can attain microscopic information related to electronic transitions and MO properties.

A goal of TDDFT excited states was to calculate absorption data and our numeric results are shown in **Table 5** and absorption spectra are shown in **Figure 4**.

Light harvesting energy (LHE) index was calculated due to its importance in electronic transfer.

The light-harvesting energy (LHE) index was calculated due to its importance in electronic transfer. In a dye sensitizer, a high LHE maximizes photo-current response, and it can be calculated with equation (1):

$$LHE = 1 - 10^{-f} \tag{1}$$

where f is the oscillator strength of the dye associated with the wavelength corresponding to the peak absorbance through intramolecular charge transfer [45, 46]. Singlet-to-singlet transitions of the absorption bands with maximum wavelength and oscillator strength were obtained for all selected anthocyanidins. In the gas-phase cyanidin had a higher LHE followed by petunidin and on the other hand, malvidin had a lower LHE value. After the addition of solvents, there is an increase in LHE in all cases but with malvidin, the effect of the solvent is more noticeable especially when methanol is used. Cyanidin, petunidin, and malvidin have higher LHE values after solvent addition. The lowest energy absorption in these molecules is due

Molecule	Solvent	State	ΔE (eV)	λ (nm)	Transition	Contribution	f	LHE
$(C_{15}H_{11}O_6)^+$	Gas Phase	1	2.546	487.1 (522*)	H -> L	67%	0.507	0.689
	Water	1	2.524	491.2	H -> L	68%	0.619	0.760
					H-1 -> L	17%		
					H-2 -> L	12%		
	Ethanol	1	2.528	490.4	H -> L	68%	0.629	0.765
					H-1 -> L	15%		
					H-2 -> L	12%		
	n-hexane	1	2.473	501.4	H -> L	69%	0.686	0.794
	Methanol	1	2.524	491.3	H -> L	68%	0.622	0.761
					H-1 -> L	17%		
					H-2 -> L	12%		
$(C_{16}H_{11}O_7)^+$	Gas Phase	1	2.448	506.4 (534*)	H -> L	61%	0.324	0.526
					H-1 -> L	30%		
					H-2 -> L	18%		
	Water	1	2.498	496.4	H -> L	68%	0.579	0.736
					H-2 -> L	17%		
	Ethanol	1	2.498	496.4	H -> L	68%	0.565	0.728
					H-2 -> L	17%		
	n-hexane	1	2.421	512.17	H-2 -> L	16%	0.574	0.733
					H -> L	68%		
	Methanol	1	2.495	496.9	H -> L	68%	0.578	0.736
					H-2 -> L	17%		
$(C_{15}H_{13}O_5)^+$	Gas Phase	1	2.312	536.4 (542*)	H -> L	60%	0.240	0.425
	Water	1	2.434	509.3	H-1 -> L	30%	0.604	0.751
	Ethanol	1	2.481	499.8	H -> L	68%	0.591	0.744
					H-2 -> L	17%		
	n-hexane	1	2.376	521.9	H -> L	70%	0.627	0.764
	Methanol	1	2.431	510.1	H -> L	61%	0.601	0.749
$(C_{15}H_{11}O_5)^+$	Gas Phase	1	2.588	479.1 (513*)	H -> L	61%	0.325	0.527
					H-1 -> L	35%		
	Water	1	2.591	478.6	H -> L	67%	0.493	0.679
					H-1 -> L	21%		
	Ethanol	1	2.592	478.4	H -> L	67%	0.472	0.663
					H-1 -> L	22%		
	n-hexane	1	2.537	488.7	H-1 -> L	24%	0.487	0.674
					H -> L	66%		
	Methanol	1	2.589	478.9	H -> L	67%	0.491	0.677
					H-1 -> L	21%		

Molecule	Solvent	State	ΔE (eV)	λ (nm)	Transition	Contribution	f	LHE
$(C_{15}H_{13}O_6)^+$	Gas Phase	1	2.401	516.3 (532*)	H -> L	67%	0.288	0.485
					H-1 -> L	11%		
	Water	1	2.509	494.2	H -> L	69%	0.530	0.705
	Ethanol	1	2.564	483.6	H -> L	67%	0.515	0.695
	n-hexane	1	2.465	503	H -> L	69%	0.535	0.708
	Methanol	1	2.505	494.9	H -> L	69%	0.527	0.703
$(C_{15}H_{12}O_6)^+$	Gas Phase	1	2.423	511.7 (543*)	H -> L	65%	0.410	0.611
	Water	1	2.460	503.9	H -> L	69%	0.600	0.749
	Ethanol	1	2.757	449.7	H-2 -> L	23%	0.682	1.792
					H -> L	66%		
	n-hexane	1	2.382	520.6	H-2 -> L	13%	0.606	0.752
					H -> L	69%		
	Methanol	1	2.458	504.5	H -> L	69%	0.599	0.748

Cyanidin, malvidin, and peonidin data has been regenerated for this work with very similar results, considering there is a set of our own results obtained with different methodology that were published previously elsewhere [22].
*Experimental data from the literature [43].

Table 5.
TD-DFT excited states absorption data for selected molecules.
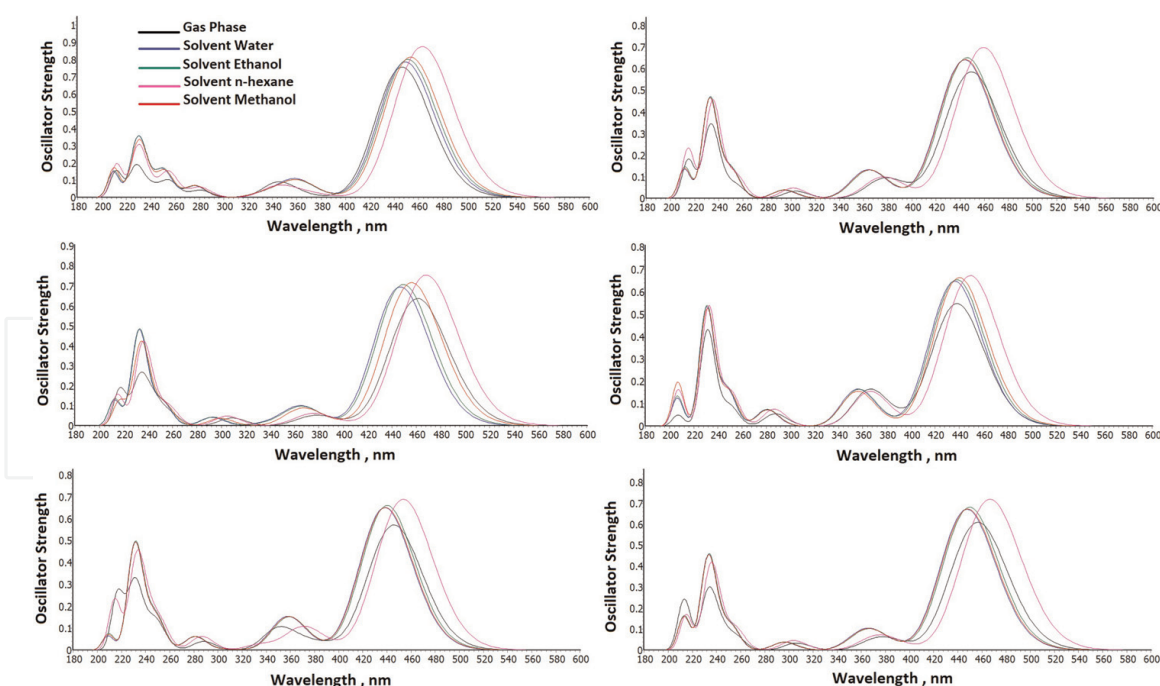
Figure 4.
Absorption spectra using TD-DFT for gas phase and solvents water, ethane, n-hexane, and methane for: (a) cyanidin [22], (b) delphinidin, (c) malvidin [22], (d) pelargonidin, (e) peonidin [22], and (f) petunidin.

to the transition from HOMO to LUMO with the largest oscillator strength resulting in an enhanced LHE, this approach emphasizes the parameters recommended in the literature to identify the best choice [41, 47, 48].

To obtain an effect where the absorption spectrum overlaps with the solar spectrum, the energy gap will have to reduce. Such action could be possible with the inclusion of a co-absorber of appropriate properties. Among the dyes studied, anthocyanidins with the higher LHE may work well with solar energy and may be recommended as the better suited for use as a potential sensitizer for DSSC.

3.5 Excited states using CIS-TDDFT

Cis-TDDFT methodology was used to calculate excited states with the scheme implemented in Gaussian16 [23]. Emission wavelength values increase after solvents are included in most cases if compared with results obtained for emission in anthocyanidins gas phase, respectively, for each variant. Emission spectra for each selected anthocyanidin are shown in **Figure 5**. According to experimental data, DFT calculations underestimate wavelength values by approximately 8%. Cyanidin, delphinidin, malvidin, and pelargonidin have similar effects with each solvent presenting slightly increased emission wavelength values for water, ethanol, and methanol and a slight decrease in wavelength value for n-hexane solvent. Peonidin and petunidin have similar effects when water and ethanol are used with a slight increase in wavelength value and are similar to the effect when used solvent n-hexane with a slight decrease but there is a different effect on these two anthocyanidins when methanol is used since, in these two variants, wavelength presents a slight decrease.

Overall, the effects of solvents in these six anthocyanidins are similar, maybe petunidin presents stronger effects in the wavelength with solvents than the others but the effects can be considered small even for this case.

Oscillator strength for the selected anthocyanidins has a particular effect for each variant that may be related to the solvent. In all cases, the gas phase displayed the lower oscillator strength value except for malvidin which presents the lower oscillator
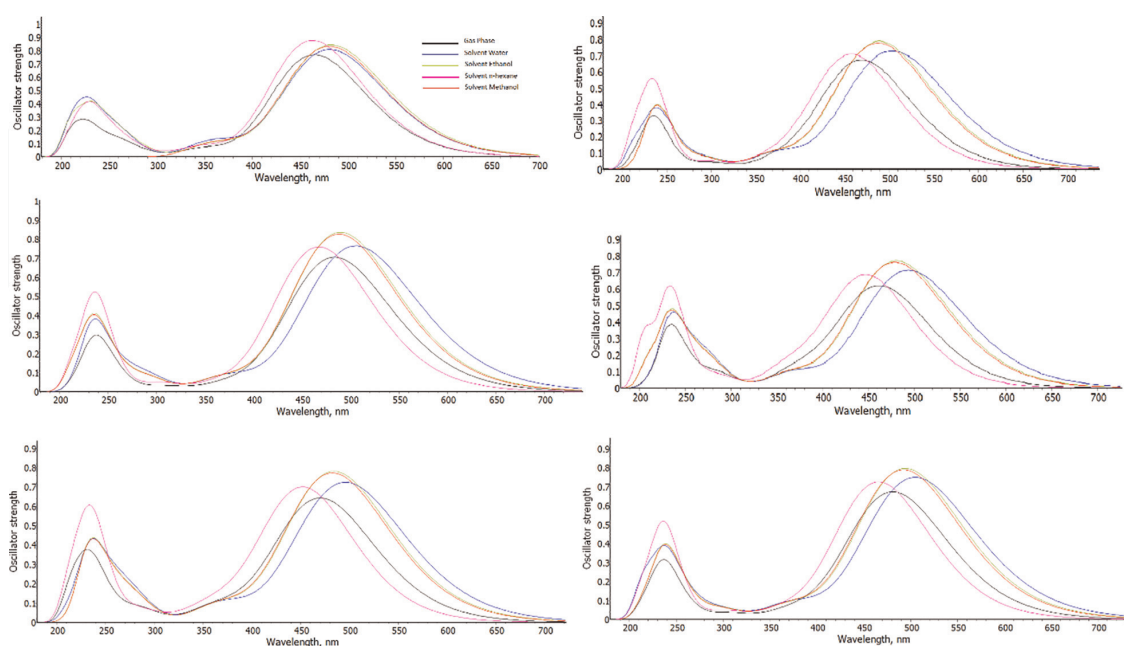

Figure 5.
Emission spectra data using TD-DFT excited states for gas phase and solvents water, ethane, n-hexane, and methane applied in the next molecules: (a) cyanidin, (b) delphinidin, (c) malvidin, (d) pelargonidin, (e) peonidin, and (f) petunidin.

strength value for the solvent methanol. In all cases, the higher oscillator strength value was observed when used solvent ethanol except for petunidin since it was with solvent water where the higher value was observed. Oscillator strength and data obtained for excited states calculations are shown in **Table 6**.

Cyanidin presented the higher oscillator strength values if compared with each anthocyanidin variant, and this behavior is maintained when the solvent is included. For cyanidin, when solvents are added the oscillator strength values increase if

Molecule	Solvent	State	ΔE (eV)	λ (nm)	Transition	Contribution	f	LHE
$(C_{15}H_{11}O_6)^+$	Gas Phase	1	2.665	465.2 (522*)	H-1 -> L	15%	0.769	1.830
					H -> L	68%		
	Water	1	2.576	481.2	H-1 -> L	13%	0.808	1.845
					H -> L	69%		
	Ethanol	1	2.569	482.7	H -> L	68%	0.877	1.867
	n-hexane	1	2.677	463.1	H -> L	68%	0.877	1.867
	Methanol	1	2.578	480.9	H-1 -> L	13%	0.832	1.853
					H -> L	69%		
$(C_{16}H_{11}O_7)^+$	Gas Phase	1	2.633	470.8 (534*)	H-2 -> L	22%	0.662	1.782
					H -> L	66%		
	Water	1	2.460	503.9	H-1 -> L	13%	0.729	1.813
					H -> L	69%		
	Ethanol	1	2.532	489.6	H -> L	69%	0.785	1.836
	n-hexane	1	2.700	459.3	H-2 -> L	24%	0.699	1.800
					H -> L	65%		
	Methanol	1	2.540	488.2	H -> L	69%	0.776	1.832
$(C_{15}H_{13}O_5)^+$	Gas Phase	1	2.561	484.2 (542*)	H -> L	67%	0.702	1.802
	Water	1	2.451	505.8	H-1 -> L	13%	0.764	1.828
					H -> L	69%		
	Ethanol	1	2.531	489.9	H-1 -> L	14%	0.835	1.854
					H -> L	69%		
	n-hexane	1	2.648	468.2	H -> L	66%	0.755	1.824
	Methanol	1	2.537	488.7	H-1 -> L	14%	0.601	1.749
					H -> L	69%		
$(C_{15}H_{11}O_5)^+$	Gas Phase	1	2.672	464.0 (513*)	H-1 -> L	18%	0.612	1.755
					H -> L	68%		
	Water	1	2.509	494.2	H -> L	70%	0.712	1.806
	Ethanol	1	2.577	481.2	H -> L	69%	0.769	1.830
	n-hexane	1	2.760	449.3	H-1 -> L	18%	0.674	1.788
					H -> L	68%		
	Methanol	1	2.586	479.5	H -> L	69%	0.760	1.826
$(C_{15}H_{13}O_6)^+$	Gas Phase	1	2.632	471.1 (532*)	H -> L	67%	0.637	1.769

Molecule	Solvent	State	ΔE (eV)	λ (nm)	Transition	Contribution	f	LHE
	Water	1	2.500	496.0	H -> L	69%	0.724	1.811
	Ethanol	1	2.560	484.4	H -> L	69%	0.779	1.834
	n-hexane	1	2.734	453.5	H -> L	66%	0.689	1.796
	Methanol	1	2.734	453.5	H -> L	66%	0.689	1.796
$(C_{15}H_{12}O_6)^+$	Gas Phase	1	2.574	481.7 (543*)	H -> L	67%	0.669	1.786
	Water	1	2.455	505.0	H -> L	69%	0.749	1.822
	Ethanol	1	2.757	449.7	H-2 -> L	23%	0.682	1.792
					H -> L	66%		
	n-hexane	1	2.657	466.7	H-2 -> L	23%	0.720	1.809
					H -> L	66%		
	Methanol	1	2.657	466.7	H-2 -> L	23%	0.720	1.748
					H -> L	66%		

Experimental data from the literature [43].

Table 6.
Excited states emission results for selected anthocyanidins using CIS-TD-DFT.

compared with its gas phase value and the higher oscillator strength values were observed with ethanol and n-hexane.

Malvidin resembles cyanidin with slightly smaller values for oscillator strength but a similar trend and in all cases when added a solvent oscillator strength, values increase aside from methanol which can be considered the only exception. Delphinidin, pelargonidin, and peonidin resemble cyanidin as well but with smaller values than malvidin so the difference with cyanidin is bigger in these cases.

Cyanidin presented the higher oscillator strength values if compared with each anthocyanidin variant and this behavior is maintained when solvent is included. For cyanidin addition of solvents cause an increase in the oscillator strength values from the gas phase value with ethanol and n-hexane having the higher oscillator strength values.

Malvidin resembles cyanidin but with smaller values for oscillator strength with a similar trend and in all cases when added solvent oscillator strength values increase with the only exception of methanol. Delphinidin, pelargonidin, and peonidin resemble cyanidin as well but with smaller values than malvidin so the difference with cyanidin is bigger in these cases. Also, in these cases, all values obtained for oscillator strength when added solvents were smaller than gas-phase oscillator strengths. For petunidin, oscillator strength changes after solvent addition are moderate, the bigger change was with the addition of water solvent.

The transition energy for the selected anthocyanidins has a similar trend among all selected after the addition of the different solvents. For cyanidin, delphinidin, malvidin, and pelargonidin transition energy for gas-phase decreases for all solvents except for n-hexane which is the only solvent where transition energy increases. For petunidin and peonidin, all the prior effects occur with the only difference that using methanol also presents an increase in the transition energy values if compared with the gas phase with similar values to those observed in n-hexane.

Also, in these cases all values obtained for oscillator strength when added solvents were smaller than gas phase oscillator strengths.

For petunidin, oscillator strength changes after solvent addition are moderate, the bigger change was with the addition of water solvent.

Transition energy for the selected anthocyanidins has a similar trend among all selected after the addition of the different solvents. For cyanidin, delphinidin, malvidin, and pelargonidin transition energy for the gas phase decreases for all solvents except for n-hexane which is the only solvent where transition energy increases. For petunidin and peonidin, all prior effects occur with the only difference that methanol also presents an increase in the transition energy values if compared with gas phase with similar values to those observed in n-hexane.

4. Conclusions

The molecule's structural geometry was analyzed a generally accepted methodology with a different basis set. Parameters such as relative angles, dihedrals, main features of individual rings, and a discussion on each molecule planarity were included as part of the discussion to relate the main geometry parameters with the molecule behavior and chemical features. Molecules functionalization with COH_3 is highlighted as an important feature for the structural and energy gap differences in each molecule geometry structure definition and is directly related with molecular orbital distribution with a direct effect in gap energy.

MOs and spectra results show there is a good fit with TiO_2 and concluded these pigments may be good dye sensitizers. Malvidin in its gas phase may be a good option from a gap energy perspective. Solvents increase their gap energy in all cases except with n-hexane which is the narrower followed by petunidin also with n-hexane. A good charge transfer feature is important as well and it was assessed with conceptual DFT. Results show cyanidin, malvidin, and pelargonidin may have a better charge transfer. A lower as possible electron reorganization energy (λ_e) and a high LHE are desirable since this would benefit charge transfer. Cyanidin has the smaller λ_e with water, but ethanol and methanol λ_e resulting values were nearly different. For LHE, the highest were cyanidin, malvidin, and petunidin with similar values between solvents. Based on our analysis of absorption capabilities for the selected pigments, it is corroborated cyanidin, malvidin, and petunidin may be acceptable dye sensitizers for DSSCs and photocatalysis applications.

Acknowledgments

Funding statement

Conflicts of interest exemption statement

Author details

Diana Barraza-Jiménez[1], Hugo Iván Flores-Hidalgo[2], Sandra Iliana Torres-Herrera[3], Raúl Armando Olvera-Corral[1] and Manuel Alberto Flores-Hidalgo[1*]

1 Scientific Computing Laboratory, Faculty of Chemistry Science, Juarez University of Durango State, Av. Veterinaria S/N, Circuito Universitario, Durango, México

2 Department of Protected and Sustainable Agriculture, Technology University of Camargo Campus Jimenez, Chihuahua, Mexico

3 Juarez University of Durango State, Faculty of Forestry Science Durango, México

*Address all correspondence to: manuel.flores@ujed.mx

IntechOpen

References

[1] Clement RC, Prasanth R. A critical review of recent developments in nanomaterials for photoelectrodes in dye sensitized solar cells. Journal of Power Sources. 2016;**317**:120-132. DOI: 10.1016/ j.jpowsour.2016.03.016

[2] Dhonde M, Sahu K, Das M, Yadav A, Ghosh P, Murty VVS. Review—recent advancements in dye-sensitized solar cells; From photoelectrode to counter electrode. Journal of The Electrochemical Society. 2022;**169**:066507

[3] Green MA et al. Solar cell efficiency tables (Version 44). Progress in Photovoltaics: Research and Applications. 2014;**22**(7):701-710. DOI: 10.1002/pip.2525

[4] O'Regan B, Grätzel M. A low-cost, high-efficiency solar cell based on dye-sensitized colloidal TiO2 films. Nature. Oct. 1991;**353**(6346):737-740. DOI: 10.1038/353737a0

[5] Dwivedi G, Munjal G, Bhaskarwar AN, Chaudhary A. Dye-sensitized solar cells with polyaniline: A review. Inorganic Chemistry Communications. 2022;**135**:109087

[6] Cole JM, Pepe G, Al Bahri OK, Cooper CB. Cosensitization in dye-sensitized solar cells. Chemical Reviews. 2019;**119** (12):7279-7327. DOI: 10.1021/acs. chemrev.8b00632

[7] Mathew S et al. Dye-sensitized solar cells with 13% efficiency achieved through the molecular engineering of porphyrin sensitizers. Nature Chemistry. 2014;**6**(3):242-247. DOI: 10.1038/ nchem.1861

[8] Roy P et al. TiO2 nanotubes and their application in dye-sensitized solar cells.

Nanoscale. 2010;**2**(1):45-59. DOI: 10.1039/b9nr00131j

[9] Hug H et al. Biophotovoltaics: Natural pigments in dye-sensitized solar cells. Applied Energy. Feb. 2014;**115**:216-225. DOI: 10.1016/j.apenergy.2013.10.055

[10] Calvin M. Solar energy by photosynthesis. Kagaku to Seibutsu. 1974;**12**(7):481-498. DOI: 10.1271/ kagakutoseibutsu1962.12.481

[11] Mohr H, Schopfer P, Hans M, Schopfer P. Wirkungen ultravioletter strahlung. Lehrbuch Der Pflanzenphysiologie. 1978:346-353. DOI: 10.1007/978-3-642-96453-4_28

[12] Lee MM et al. Efficient hybrid solar cells based on meso-superstructured organometal halide perovskites. Science. 2012;**338**(6107):643-647. DOI: 10.1126/ science.1228604

[13] Norris DJ, Aydil ES. Getting moore from solar cells. Science. 2012;**338** (6107):625-626. DOI: 10.1126/ science.1230283

[14] Hagfeldt A. Brief overview of dye-sensitized solar cells. AMBIO. 2012;**41** (S2):151-155. DOI: 10.1007/s13280-012-0272-7

[15] Woodford JN. A DFT investigation of anthocyanidins. Chemical Physics Letters. 2005;**410**(4):182-187. DOI: 10.1016/j.cplett.2005.05.067

[16] Estévez L, Mosquera RA. First characterization of the formation of anthocyanin–Ge and anthocyanin–B complexes through UV–Vis spectroscopy and density functional theory quantum chemical calculations. Journal of Agricultural and Food Chemistry. 2021;

69(4):1272-1282. DOI: 10.1021/acs.jafc.0c06827

[17] Castañeda-Ovando A, Pacheco-Hernández Md L, Páez-Hernández ME, Rodríguez JA, Galán-Vidal CA. Chemical studies of anthocyanins: A review. Food Chemistry. 2009;**113**:859-871

[18] Cavalcanti RN et al. Non-thermal stabilization mechanisms of anthocyanins in model and food systems —An overview. Food Research International. 2011;**44**(2):499-509. DOI: 10.1016/j.foodres.2010.12.007

[19] Francis F. Chapter 12 - Food colorings. In: Douglas B, editor. Published in Book: Color in Food. CRC Press: MacDougall. Woodhead Publishing; 2002. p. 297

[20] Kalt W et al. Anthocyanin content and profile within and among blueberry species. Canadian Journal of Plant Science. 1999;**79**(4):617-623. DOI: 10.4141/p99-009

[21] Davies KM. Chapter: Modifying anthocyanin production in flowers, published in book: Anthocyanins: Biosynthesis, Functions, and Applications. In: Gould K, Davies K, Winefield C, editors. Science+Business Media LLC. 2009

[22] Barraza-Jiménez D, Flores-Hidalgo MA, et al. Solvent effects on dye sensitizers derived from anthocyanidins for applications in photocatalysis. In: Glossman-Mitnik MD, Maciejewska M, editors. Chapter Published in Book: Solvents, Ionic Liquids and Solvent Effects. London, UK: IntechOpen; 2019

[23] Frisch MJ, Fox DJ, et al. Gaussian 16, Revision C.01. Wallingford CT: Gaussian, Inc.; 2016

[24] Becke AD. Density-functional thermochemistry III. The role of exact exchange. The Journal of Chemical Physics. 1993;**98**:5648

[25] Terranova U, Bowler DR. Δ Self-consistent field method for natural anthocyanidin dyes. Journal of Chemical Theory and Computation. 2013;**9**(7): 3181-3188. DOI: 10.1021/ct400356k

[26] Fan W, Deng W. Incorporation of thiadiazole derivatives as π-spacer to construct efficient metal-free organic dye sensitizers for dye-sensitized solar cells: A theoretical study. Communications in Computers & Chemistry. 2013;**1**:152-170. DOI: 10.4208/cicc.2013.v1.n2.6

[27] Armas R, Miguel M, Oviedo J, Sanz JF. Coumarin derivatives for dye sensitized solar cells: A TD-DFT study. Physical Chemistry Chemical Physics. 2012;**14**:225. DOI: 10.1039/C1CP22058F

[28] Baldenebro-López J et al. Density functional theory (DFT) study of triphenylamine-based dyes for their use as sensitizers in molecular photovoltaics. International Journal of Molecular Sciences. 2012;**13**(4, 1):4418-4432. DOI: 10.3390/ijms13044418

[29] Xu J et al. DFT Studies on the electronic structures of indoline dyes for dye-sensitized solar cells. Journal of the Serbian Chemical Society. 2010;**75**:259

[30] Leonid S. Chemissian. V4.43. pp. 2005-2016

[31] Ge X, Xiaochuan, et al. Accurate and inexpensive prediction of the color optical properties of anthocyanins in solution. The Journal of Physical Chemistry A. 2015;**119**(16):3816-3822. DOI: 10.1021/acs.jpca.5b01272

[32] Woodford JN, Li W. Recent progress of thin-film photovoltaics for indoor application. Chinese Chemical Letters. 2020;**31**:643

[33] Buseta PB, Colleter JC, Gadret M. Structure du chlorure d'apigéninidine monohydrate. Acta Crystallographica B. 1974;**30**:1448

[34] Ueno K, Saito N, Ueno K, Saito N. Cyanidin bromide monohydrate (3,5,7,3',4'-pentahydroxyflavylium bromide monohydrate). Acta Crystallographica Section B: Structural Crystallography and Crystal Chemistry. 1977;**33**(1):114-116. DOI: 10.1107/ S0567740877002702

[35] Meyer M. Ab initio study of flavonoids. International Journal of Quantum Chemistry. 2000;**76**(6):724-732

[36] Sanchez-Bojorge NA et al. Theoretical calculation of the maximum absorption wavelength for Cyanidin molecules with several methodologies. Computational and Theory of Chemistry. 2015;**1067**:129-134

[37] Liu Z. Theoretical studies of natural pigments relevant to dye-sensitized solar cells. Journal of Molecular Structure: THEOCHEM. 2008;**862**:44. DOI: 10.1016/j.theochem.2008.04.022

[38] Sánchez de Armas R, San-Miguel MA, Oviedo J, Sanz J. Direct vs. indirect mechanisms for electron injection in DSSC: Catechol and alizarin. Computational Theory of Chemistry. 2011;**975**:99

[39] Glossman-Mitnik D. Computational molecular characterization of Coumarin-102. Journal of Molecular Structure: THEOCHEM. 2009;**911**:105

[40] Mohammadi N, Wang F. First-principles study of Carbz-PAHTDDT dye sensitizer and two carbz-derived dyes for dye sensitized solar cells. Journal of Molecular Modeling. 2014;**20**: 2177

[41] Megala M, Rajkumar BJM. Theoretical study of anthoxanthin dyes for dye sensitized solar cells (DSSCs). Journal of Computational Electronics. 2016;**15**(557). DOI: 10.1007/s10825-016-0791-8

[42] Harborne JB, Harborne JB. Comparative biochemistry of flavonoids. The Biochemical Journal. 1958;**V70**:22

[43] Brouillard R. The Mechanism of Co-Pigmentation of Anthocyanins in Aqueous Solutions. London: Chapman and Hall Ltd.; 1988. p. 525

[44] El Kouari Y, Migalska-Zalas A, Arof AK, Sahrao B. Computations of absorption spectra and nonlinear optical properties of molecules based on anthocyanidin structure. Optical and Quantum Electronics. 2015;**47**:1091-1099

[45] Roy P, Kumar Sinha NK, Tiwari S, Khare A. A review on perovskite solar cells: Evolution of architecture, fabrication techniques, commercialization issues and status. Solar Energy. 2020;**198**:665

[46] Zhang CR et al. The role of the conjugate bridge in electronic structures and related properties of tetrahydroquinoline for dye sensitized solar cells. H.S. Chen. International Journal of Molecular Sciences. 2013;**14**: 5461

[47] Abdullah MI, Janjua MRSA, Mahmood A, Ali S, Ali M, Abdullah B, et al. Quantum chemical designing of efficient sensitizers for dye sensitized solar cells. Bulletin of the Korean Chemical Society. 2013;**34**(7):2093-2098. DOI: 10.5012/bkcs.2013.34.7.2093

[48] Chien CY, Hsu BD. Optimization of the dye-sensitized solar cell with anthocyanin as photosensitizer. Solar Energy. 2013;**98**:203-211